Hard Photons from a Non-Equilibrated Quark–Gluon Plasma with Finite Baryon Density at a Two-Loop Level

2005 Chinese Phys. Lett. 22 2519

(http://iopscience.iop.org/0256-307X/22/10/017)

Hard Photons from a Non-Equilibrated Quark–Gluon Plasma with Finite Baryon Density at a Two-Loop Level *

HE Ze-Jun(贺泽君)[1,2], LONG Jia-Li(龙家丽)[1,3], MA Yu-Gang(马余刚)[1,2]

[1] *Shanghai Institute of Applied Physics, Chinese Academy of Sciences, PO Box 800-204, Shanghai 201800*

[2] *CCAST (World Laboratory), PO Box 8730, Beijing 100080*

[3] *Graduate School of the Chinese Academy of Sciences, Beijing 100049*

(Received 13 April 2005)

We study hard photon production from a two-loop level (bremsstrahlung and annihilation with scattering) in a chemically equilibrating quark–gluon plasma at finite baryon density based on Jüttner distribution of partons of the system. We find that the photon yield from the two-loop level increases obviously with the increasing initial quark chemical potential.

PACS: 12. 38. Mh, 25. 75. −q, 24. 85. +p

The study of single photon production at relativistic heavy ion collisions has gained momentum in recent years due to availability of experimental data from CERN, SPS and also the data expected shortly from the RHIC experiments at BNL.[1] Hard photons are a promising probe for the detection of the quark-gluon plasma (QGP) created in ultrarelativistic heavy ion collisions. Because of the large mean-free path of photons and the dependence of photon production on the thermodynamical condition of the QGP, photons produced in the QGP carry information on the thermodynamical state at the moment of their production.[2,3] Previous authors have studied the production of hard photons in a QGP at finite temperature.[2] Assuming the formation of a QGP already at AGS and SPS energies, however, a finite chemical potential μ_q has to be considered[4] and even at RHIC energies the quark chemical potential μ_q may not be negligible as indicated by RQMD simulation ($\mu_q \approx 1 - 2T$).[5]

Recently, Hammon, Geiger and their co-workers[6,7] have indicated that the initial QGP system produced at the RHIC energies has finite baryon density, Majumder and Gale[8] have discussed the dileptons from QGP produced at the RHIC energies at finite baryon density, and Bass *et al.*[9] have pointed out that the parton rescattering and fragmentation lead to a substantial increase in the net-baryon density at midrapidity over the density produced by initial primary parton-parton scatterings. These show that one may further study the effect of the quark chemical potential on the signature of the QGP formation. At a given energy density, the lowest-order-perturbation-theory estimations indicate a strong suppression of the photon production at non-vanishing quark chemical potential μ_q as compared to the case $\mu_q = 0$.[10] Traxler *et al.* have computed the photon production rate of a QGP at finite quark chemical potential for a given temperature (also a given energy density) using the Braaten–Pisarski method.[11] In addition, Traxler and co-workers[12,13] have studied the photon production in a chemically equilibrating baryon-free QGP system. Recently, the work of Aurenche *et al.*[14] shows that the two-loop process bremsstrahlung generates contributions of the same order of magnitude as those calculated by several groups at one loop. It is necessary to study the two-loop contributions of photon production in a chemically equilibrating QGP system at finite baryon density.

In this work, we study the hard photon production from the two-loop processes in a chemically equilibrating QGP system at finite baryon density to reveal the effect of the quark chemical potential on the production. As pointed out in Ref. [15] that it is difficult to study the whole process of the chemical equilibration of the system based on the previous approximation distribution functions of partons. We describe the evolution and photon production of a chemically equilibrating QGP system at finite baryon density on the basis of the Jüttner distribution function of partons. We generalize the approach of Refs. [1,14] to the Jüttner distribution of partons at finite baryon density, and describe the evolution of the system as carried out in Refs. [15,16].

Expanding densities of quarks (anti-quarks) over quark chemical potential μ_q, we can obtain the baryon density of the system and the corresponding energy density. We consider the reactions leading to chemical equilibrium not only $gg \rightleftharpoons ggg$ and $gg \rightleftharpoons q\bar{q}$ but also $gg \rightleftharpoons s\bar{s}$ and $q\bar{q} \rightleftharpoons s\bar{s}$. Assuming that elastic parton scatterings are sufficiently rapid to maintain the local thermal equilibrium, the evolutions of gluon,

* Supported in part by the Knowledge Innovation Project of Chinese Academy of Sciences under Grant No KJCX2-N11, the National Natural Science Foundation of China under Grant Nos 10405031, 10275002, 10328509 and 10135030, the Major State Basic Research and Development Programme of China under Grant No G200077400.

** Email: hezejun@sinap.ac.cn

quark and s quark density can be given by their master equations, respectively. Combining these master equations with equations of baryon number and energy–momentum conservation, we can obtain the evolution equations of the system. We solve this set of equations to obtain evolutions of the system for a set of initial conditions.

The earlier works[12,17,18] considered the hard photon production due to annihilation $q\bar{q} \to g\gamma$ and QCD Compton ($qg \to q\gamma$ and $\bar{q}g \to \bar{q}\gamma$) scattering processes from a quark matter which appear at the one-loop level in the effective theory, as performed in Ref. [19]. Recently, it is shown by calculations of Refs. [1,14,20,21] that significant contribution also comes from the bremsstrahlung and a new process called the annihilation with scattering (AWS) that arises at the two-loop level in the effective theory. The authors of Refs. [1,14] have studied the hard photon production from the bremsstrahlung and AWS process in the framework of hard thermal loop resummed effective field theory. Especially the authors of Ref. [22] have considered finite baryon density, but they did not include it in their final calculation. In this work, we extend their expressions to estimate the photon production rates from the bremsstrahlung and AWS process at finite baryon density. Since they in the final calculation only consider the photon production from the baryon-free QGP system, the contribution from quarks is equal to the one from anti-quarks. Thus they only study the contribution from quarks and multiply it by a factor 2 to obtain the total bremsstrahlung photon yield. However, for a QGP system at finite baryon density the contribution from quarks differs from the one from anti-quarks. Thus, we should first multiply the right-hand side of Eq. (43) in Ref. [22] by a factor 1/2, then add the contribution from anti-quarks to obtain the total bremsstrahlung photon yield. Thus from Eqs. (43) and (45) of Ref. [22], we have the production rate for the bremsstrahlung process

$$\left(E\frac{dR}{d^3p}\right)_{\rm brem} = \frac{NC_F\alpha\alpha_s}{\pi^5}(\Sigma e_f^2)\frac{T}{E^2}(J_T - J_L) \cdot \frac{\lambda_g}{e^{E/T} - \lambda_g}\int_0^\infty dp(p^2 + (p+E)^2) \cdot \left[\left(\frac{\lambda_q}{e^{(p-\mu_q)/T} + \lambda_q} + \frac{\lambda_q}{e^{(p+\mu_q)/T} + \lambda_q}\right) - \left(\frac{\lambda_q}{e^{(p+E-\mu_q)/T} + \lambda_q} + \frac{\lambda_q}{e^{(p+E+\mu_q)/T} + \lambda_q}\right)\right] \quad (1)$$

and for the AWS process

$$\left(E\frac{dR}{d^3p}\right)_{AWS} = \frac{NC_F\alpha\alpha_s}{\pi^5}(\Sigma e_f^2)\frac{T}{E^2}(J_T - J_L) \cdot \frac{\lambda_g}{e^{E/T} - \lambda_g}\int_0^E dp(p^2 + (E-p)^2) \cdot \left[\frac{\lambda_q}{e^{(p+\mu_q)/T} + \lambda_q} - \frac{\lambda_q}{e^{(E+p+\mu_q)/T} + \lambda_q}\right], \quad (2)$$

where e_f is the electric charge of the quark flavour f in units of electron charge, and α is the fine-structure constant, the running coupling constant $\alpha_s = 0.4$. In Eq. (2), the p-integral is carried out from 0 to E as phase space is restricted in the range $0 \le p \le E$. In addition, as carried out in Ref. [22] using asymptotic thermal quark mass $M_\infty^2 = 2m_q^2$, and thermal gluon mass m_g^2 we have calculated factors J_T and J_L. For our system, m_q^2 and m_g^2 are, respectively, given by

$$m_q^2 = \frac{4\alpha_s}{3\pi}T^2\left[2(G_1^1\lambda_g + Q_1^1\lambda_q) + \left(\frac{\mu_q}{T}\right)^2\frac{\lambda_q}{\lambda_q + 1}\right], \quad (3)$$

and

$$m_g^2 = \frac{4\alpha_s}{3\pi}T^2\left\{6G_1^1\lambda_g + N_f\left[2Q_1^1\lambda_q + \left(\frac{\mu_q}{T}\right)^2\frac{\lambda_q}{\lambda_q + 1}\right]\right\}. \quad (4)$$

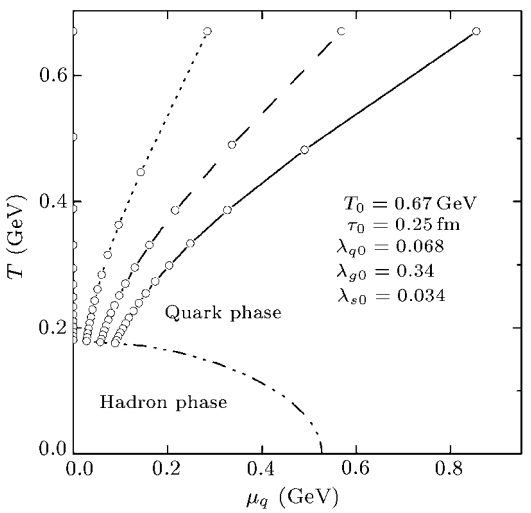

Fig. 1. The calculated evolution paths of the system in the phase diagram for initial values $\tau_0 = 0.25$ fm, $T_0 = 0.67$ GeV, $\lambda_{g0} = 0.34$, $\lambda_{q0} = 0.068$ and $\lambda_{s0} = 0.034$, where the dash-dotted, dotted, dashed and solid lines are, in turn, the evolution paths for initial quark chemical potentials $\mu_{q0} = 0.000,\ 0.284,\ 0.568,\ 0.852$ GeV, and the dot-dot-dashed line is the phase boundary of the phase diagram. The time interval between the two small circles is 0.3 fm (i.e., 30× calculation-step 0.01 fm). The phase diagram is calculated at $B^{1/4} = 0.25$ GeV.

We further integrate these photon production rates over the spacetime volume of the reaction. According to Bjorken's model, the volume element $d^4x = d^2x_T dy\tau d\tau$, where τ is the evolution time of the system and y the rapidity of the fluid element. We consider central collisions of $A_u^{197} + A_u^{197}$ so the integration over transverse coordinates just yields a factor of $d^2x_T = \pi R_A^2$, where R_A is the nuclear radius. We

finally obtain the photon spectra

$$\frac{dn}{d^2p_T} = \pi {R_A}^2 \int_{\tau_0}^{\tau_{fin}} \tau d\tau \int_{-y_{flu}}^{y_{flu}} dy \int_0^{Y_{\max}} dY \cdot \left(E\frac{dn}{d^3pd^4x}\right), \quad (5)$$

where Y is the rapidity of photons, the rapidity of the fluid is $y_{flu} = 6$ as taken in Ref. [12] the rapidity of the photon is taken up to $Y_{\max} = 6$, τ_{fin} is the evolution time which the QGP system reaches the phase boundary from initial state.

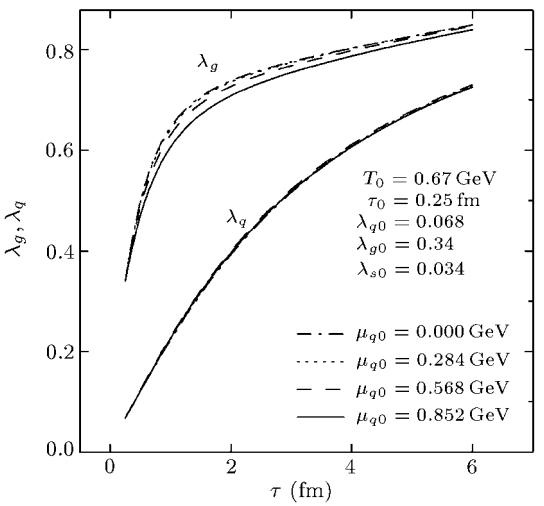

Fig. 2. The calculated equilibration rates at the same initial conditions as given in Fig. 1. The gluon and quark equilibration rates are, in turn, denoted by the λ_g and λ_q. The dot-dashed, dotted, dashed and solid lines denote, respectively, the equilibration rates for initial quark chemical potentials $\mu_{q0} = 0.000$, 0.284, 0.568, 0.852 GeV.

We focus on discussion Au^{197}+Au^{197} central collisions at the RHIC energies. We take initial values from the self-screened parton cascade (SSPC) model: $\tau_0 = 0.25$ fm, $T_0 = 0.67$ GeV, $\lambda_{g0} = 0.34$, $\lambda_{q0} = 0.068$ and $\lambda_{s0} = 0.034$. The calculated evolution paths of the system in the phase diagram have been shown in Fig. 1. The dot-dashed, dotted, dashed and solid lines are, in turn, the evolution paths for initial quark chemical potentials $\mu_{q0} = 0.000$, 0.284, 0.568, 0.852 GeV, and the dot-dot-dashed line the phase boundary of the phase diagram. The time interval between the two small circles is 0.3 fm (i.e., 30×calculation-step 0.01 fm). The phase diagram is calculated at the bag constant $B^{1/4} = 0.25$ GeV. We can see the effect of the finite initial quark chemical potential on the evolution of the system from Fig. 1. As described in Ref. [15] the increase of the initial quark chemical potential will change the hydrodynamic behaviour of the system to cause the increase of the quark phase lifetime, making the evolution of the system become slower towards reaching the phase boundary. In Fig. 2 we give the calculated equilibration rates at the same initial conditions as given in Fig. 1. The dot-dashed, dotted, dashed and solid lines denote, respectively, the equilibration rates for initial quark chemical potentials $\mu_{q0} = 0.000$, 0.284, 0.568, 0.852 GeV. Figure 2 shows that both the chemical equilibration rates λ_g of gluons and λ_q of quarks increase rapidly with the evolution time and that the chemical equilibration rate of gluons decreases with the increasing initial quark chemical potential.

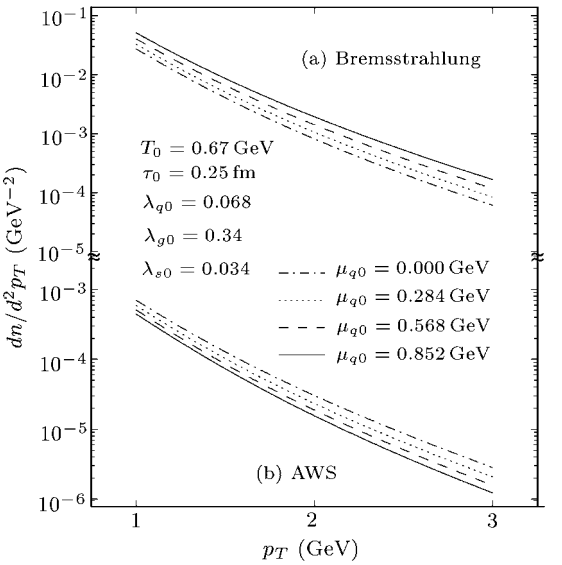

Fig. 3. The calculated photon spectra for (a) the bremsstrahlung and (b) the annihilation with scattering processes. The dot-dashed, dotted, dashed and solid lines are, respectively, the calculated spectra for initial quark chemical potentials $\mu_{q0} = 0.000$, 0.284, 0.568, 0.852 GeV based on the evolution described in Fig. 1.

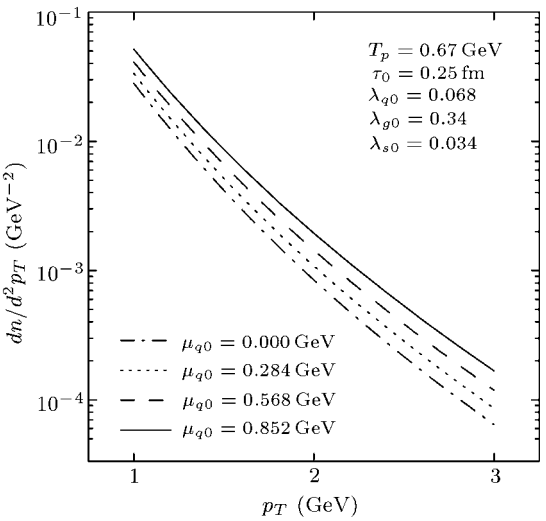

Fig. 4. The total two-loop photon spectra. The dot-dashed, dotted, dashed and solid lines are, respectively, the calculated total photon spectra for initial quark chemical potentials $\mu_{q0} = 0.000$, 0.284, 0.568, 0.852 GeV based on the evolution described in Fig. 1.

The calculated photon spectra for the bremsstrahlung and AWS processes are given in (a)

and (b) panels of Fig. 3. The total two-loop photon spectra are shown in Fig. 4. The dot-dashed, dotted, dashed and solid lines in Figs. 3 and 4 are, respectively, the calculated spectra for initial quark chemical potentials $\mu_{q0} = 0.000,\ 0.284,\ 0.568,\ 0.852$ GeV. With the increase of the quark chemical potential, the anti-quark density decreases, thus the photon production for AWS process calculated from Eqs. (2) also decrease. It is well known that the baryon-free QGP converts into the hadronic matter only with the decreasing temperature along the temperature axis of the phase diagram, and the phase transition occurs at a certain critical temperature T_c. However, in this work, both the quark chemical potential and the temperature of the system are functions of time, compared with the baryon-free QGP it necessarily takes a long time (also a long path) for value (μ_q, T) of the system to reach a certain point of the phase boundary to make the phase transition. Furthermore, in the calculation we have found that with the increasing initial quark chemical potential, the production rate of gluons increases, and thus the gluon equilibration rate decreases (see Fig. 2), leading to the little energy consumption of the system, i.e. slow cooling of the system. Since gluons are much more than quarks in the system, overall with the increasing initial quark chemical potential, the cooling of the system further slows down. These cause the quark phase lifetime to further increase. These evolution features of the system can be clearly seen in Fig. 1. With the help of the calculation of Eq. (5), one can note that these factors strongly heighten the contribution of the integration over the evolution of the system to the photon production and can compensate for the photon suppression. One also knows that since the quark density increases and the anti-quark density decreases with the increase of the quark chemical potential, the photon production calculated by Eqs. (1) for bremsstrahlung increases, and by Eqs. (2) for the AWS process decreases. The calculations of Eq. (5) have shown that due to the effect of the evolution of the system, with increasing the initial quark chemical potential the increase of the photon production for bremsstrahlung become even faster, and the decrease of the photon production for the AWS process obviously decreases, as seen in panels (a) and (b) of Fig. 3, respectively. In the calculation, we have found that the contribution of the bremsstrahlung obviously increases with the increase of the initial quark chemical potential, and its contribution dominates. Due to the bremsstrahlung, the total two-loop photon spectrum of the QGP system rises far faster with the increasing initial quark chemical potential. Finally, we can see that the total two-loop photon spectra in Fig. 4 is a strongly increasing function of the initial quark chemical potential.

In conclusion, we have found that the increase of the initial quark chemical potential changes the hydrodynamic behaviour of the system to cause the quark phase lifetime to increase. This effect is to heighten the photon yield of the bremsstrahlung and AWS processes, and can compensate for the photon suppression effect of the AWS process caused by the increase of the initial quark chemical potential, making the total two-loop photon yield as a strongly increasing function of the initial quark chemical potential. It is shown that the bremsstrahlung is a main process making the total two-loop photon yield as a strongly increasing function of the initial quark chemical potential.[21] In addition, compared with previous results from the one-loop process, we find that the two-loop contributions to the photon production seem to dominate over the one-loop processes.

References

[1] Matsui T and Satz H 1986 *Phys. Lett.* B **178** 416
[2] Rafelski J and Müller B 1982 *Phys. Rev. Lett.* **48** 1066
[3] Shuryak E 1980 *Phys. Rep.* **80** 71
[4] Kajantie K, Kapusta J, McLerran L and Mekjian A 1986 *Phys. Rev.* D **34** 2746
[5] Dumitru A, Rischke D H and Schönfeld Th et al 1993 *Phys. Rev. Lett.* **70** 2860
[6] Hammon N, Stöcker H and Greiner W 1999 *Phys. Rev.* C **61** 014901
[7] Geiger K and Kapusta J I 1993 *Phys. Rev.* D **47** 4905
[8] Majumder A and Gale C 2001 *Phys. Rev.* D **63** 114008
[9] Bass S A, Müller B and Srivastava D K 2003 *Phys. Rev. Lett.* **91** 052302
[10] Dumitru A, Rischke D H and Stöcker et al 1993 *Mod. Phys. Lett.* A **8** 1291
[11] Traxler C T, Vija H and Thoma M H 1995 *Phys. Lett.* B **346** 3294
[12] Traxler C T and Thoma M H 1996 *Phys. Rev.* C **53** 1348
[13] Strickland M 1994 *Phys. Lett.* B **331** 245
[14] Aurenche P, Gelis F et al 1998 *Phys. Rev.* D **58** 085003
[15] He Z J, Long J L, Ma Y G, Ma G L and Liu B 2004 *Phys. Rev.* C **69** 034906
[16] He Z J, Long J L, Ma Y G et al 2004 *Chin. Phys. Lett.* **21** 795
[17] Kapusta J, Lichard P and Seibert D 1991 *Phys. Rev.* D **44** 2774
[18] Baier R, Nakkagawa H, Neigawa A and Redlich K 1992 *Z. Phys.* C **53** 433
[19] He Z J, Long J L, Ma Y G et al 2005 *Chin. Phys. Lett.* **22** 1350
[20] Arnold P, Moore G D and Yaffe L G 2001 *J. High Energy Phys.* **11** 057
[21] Arnold P, Moore G D and Yaffe L G 2001 *J. High Energy Phys.* **12** 09
[22] Dutta D, Sastry S V S, Mohanty A K et al 2002 *Nucl. Phys.* A **710** 415